Particle Accelerators
1975, Vol. 6, pp. 77–82

SECOND-ORDER APPROXIMATION OF ELECTRON TRAJECTORIES IN HIGH ENERGY RESOLUTION LINAC

Y. TAKEUCHI, H. FUJIOKA, AND K. URA

Electron Beam Laboratory, Faculty of Engineering, Osaka University, Yamada-Kami, Suita, Osaka, 565, Japan

(*Received October 29, 1973; in final form December 26, 1973*)

For electron beams injected into a linac at the optimum injection phase, the energy variation at the exit plane depends on the variation of the injection energy to the first order, while it depends on the injection phase width and the transverse injection conditions to the second order. In this report, we shall show the systematic procedure to make the second-order correction by aberration coefficients which are calculated from the direct integration of the second-order trajectory equations. It is proved that the invariance of the normalized longitudinal emittance extends to the second-order approximation for the axial electrons, provided that the relative variation of the injection energy is sufficiently smaller than that of the injection phase width. Finally, some numerical examples are given and discussed.

1 INTRODUCTION

The linear or paraxial approximation is often employed in the analysis of trajectories in linacs or other particle accelerators. For instance, Septier and Boussoukaya studied the properties of paraxial trajectories in the linac with a variable phase velocity,[1,2] and also reported some examples which show numerically the invariance of the normalized transverse emittance of paraxial electron beams.[3] We also have reported the analytical invariances of the longitudinal and the transverse normalized emittances of paraxial electron beams in the rotationally symmetrical TM rf electromagnetic fields.[4]

At the optimum injection phase, however, the paraxial approximation can not describe the relation between the output energy and the injection phase width or other injection conditions which is important in the case of high energy resolution linacs. In this case, the second-order approximation is necessary. Indeed, Boussoukaya and Septier derived the second-order longitudinal trajectory equation satisfied by the axial electron near by the peak of the accelerating electric field in a traveling-wave linac. They integrated, however, the original complete longitudinal trajectory equation instead of the above second-order equation, and deduced the relation between an output energy and an injection phase in the case of axial electrons.[2]

When one approximates the longitudinal and the transverse trajectories of electrons moving through rf electromagnetic fields, higher-order approximation than the second order can be treated as aberrations.[5] Although Boussoukaya and Septier analyzed the relation between the variation of output energy and the injection conditions, longitudinal or transverse, they do not stand on this point. Matsuda and Ura reported the general formulation with integral forms on the second-order and the third-order aberration coefficients, and applied them to the TM_{010}-cavity with small beam-limiting apertures.[6]

In this paper, we shall show the systematic procedure to estimate the second-order aberration coefficients by direct integration of the 2nd-order trajectory equations. We shall next discuss the invariance of the normalized longitudinal emittance, and show some numerical examples.

2 LONGITUDINAL AND TRANSVERSE TRAJECTORY EQUATIONS

We choose the beam axis as the z-axis and assume the cylindrical TM-mode without space charges and static magnetic fields. Then, the longitudinal trajectory equation representing phase motions $\omega t(z)$, and the transverse trajectory equation satisfied by the off-axis coordinate $r(z)$ are given as

follows,

$$c/k \cdot t'' + \{(ct')^2 - 1 - r'^2\}^{1/2} \cdot [-\{(ct')^2 - 1\}\eta E_z/kc^2 - ct'r'\eta B_\phi/kc + r'\eta E_r/kc^2] = 0, \quad (1)$$

$$1/k \cdot r'' + \{(ct')^2 - 1 - r'^2\}^{1/2} \cdot \{-ct'r'\eta E_z/kc^2 - (r'^2 + 1)\eta B_\phi/kc + ct'\eta E_r/kc^2\} = 0, \quad (2)$$

where $k = \omega/c$, ω is the angular frequency, $-\eta$ the ratio of the charge $-e$ to the rest mass m of an electron, and prime and double prime indicate derivatives with respect to the coordinate z.

We now expand the variables t and r in a perturbation parameter $\tilde{\omega}$ as follows,

$$\left.\begin{aligned} t &= T + \tilde{\omega}\tau_1 + \tilde{\omega}^2\tau_2 + \cdots \\ r &= \tilde{\omega}r_1 + \tilde{\omega}^2 r_2 + \cdots \end{aligned}\right\}. \quad (3)$$

In the above expansion, $T(z)$ is the reference longitudinal trajectory of the electron which can be chosen arbitrarily. $\tau_1(z)$ and $r_1(z)$ means the paraxial trajectories. $\tau_2(z)$ and $r_2(z)$ are the second-order aberrations. The field components E_z, E_r and B_ϕ of cylindrically symmetric TM modes can be expressed as a function of the axial electric field $E_z(t = T, r = 0, z)$ and be expanded in terms of r_1, r_2, τ_1 and τ_2 as shown in the Appendix. The effects of the radial field variation and the space harmonics are included in the following treatment. The kinetic energy can be also expanded likewise as follows,

$$K = K_0 + \tilde{\omega}K_1 + \tilde{\omega}^2 K_2 + \cdots, \quad (4)$$

where

$$\begin{aligned} K_0 &= mc^2[cT'\{(cT')^2 - 1\}^{-1/2} - 1], \\ K_1 &= -mc^2\{(cT')^2 - 1\}^{-3/2}c\tau_1', \\ K_2 &= mc^2[3/2 \cdot \{(cT')^2 - 1\}^{-5/2}cT'(c\tau_1')^2 \\ &\quad + 1/2 \cdot \{(cT')^2 - 1\}^{-3/2}cT'r_1'^2 \\ &\quad - \{(cT')^2 - 1\}^{-3/2}c\tau_2']. \end{aligned} \quad (5)$$

For convenience in the following discussion, the next expressions are defined:

$$K_1/K_0 = \kappa c\tau_1', \quad (6)$$

$$K_2/K_0 = \lambda(c\tau_1')^2 + \mu r_1'^2 + \kappa c\tau_2'. \quad (7)$$

2.1 *Reference Trajectory Equation*

The reference trajectory equation can be obtained by substituting Eq. (3) into Eqs. (1) and (2), and by picking up the zeroth-order terms:

$$c/k \cdot T'' = \{(cT')^2 - 1\}^{3/2}\eta a_0/kc^2, \quad (8)$$

$$a_0 = E_z(t = T, r = 0, z). \quad (9)$$

2.2 *Paraxial Trajectory Equations*

The paraxial trajectory equations can be obtained by picking up the first-order terms of the series expansion of Eqs. (1) and (2):

$$c/k \cdot \tau_1'' - 3\{(cT')^2 - 1\}^{1/2}cT'\eta a_0/kc^2 \cdot c\tau_1' - \{(cT')^2 - 1\}^{3/2}\eta/kc^2 \cdot \partial a_0/\partial T \cdot \tau_1 = 0, \quad (10)$$

$$1/k \cdot r_1'' - \{(cT')^2 - 1\}^{1/2}\eta/kc^2 \cdot \{cT'a_0 r_1' + 1/2 \cdot (cT'\partial a_0/\partial z + \partial a_0/\partial T \cdot 1/c)r_1\} = 0. \quad (11)$$

It should be remarked here that the paraxial properties of the longitudinal trajectory are independent of the transverse one. $c\tau_1'$ and $\omega\tau_1$ at the exit plane which can be chosen arbitrarily are connected with those at the injection plane by the longitudinal transformation matrix (L_{jk}):

$$\begin{pmatrix} c\tau_1' \\ \omega\tau_1 \end{pmatrix} = \begin{pmatrix} L_{11} & L_{12} \\ L_{21} & L_{22} \end{pmatrix} \begin{pmatrix} c\tau_{1i}' \\ \omega\tau_{1i} \end{pmatrix}, \quad (12)$$

where the subscript i means the injection plane. If the reference electron is injected at the optimum phase for which the output energy reaches a maximum, then the component L_{12} vanishes.

The paraxial transverse trajectory satisfying Eq. (11) is given in the same way as the longitudinal case by,

$$\begin{pmatrix} r_1' \\ kr_1 \end{pmatrix} = \begin{pmatrix} M_{11} & M_{12} \\ M_{21} & M_{22} \end{pmatrix} \begin{pmatrix} r_{1i}' \\ kr_{1i} \end{pmatrix}. \quad (13)$$

The component M_{21} will vanish at the image plane and M_{22} vanishes at the cross-over plane.

2.3 *Trajectory Equations of the Second Order*

The trajectory equations of the second order can be obtained by picking up the second-order terms of the series expansion of Eqs. (1) and (2):

$$c/k \cdot \tau_2'' - 3\{(cT')^2 - 1\}^{1/2}cT'\eta a_0/kc^2 \cdot c\tau_2' - \{(cT')^2 - 1\}^{3/2}\eta/kc^2 \cdot \partial a_0/\partial T \cdot \tau_2 = \sum_{j=1}^{6} c_j, \quad (14)$$

where

$$
\begin{aligned}
c_1 &= \{(cT')^2 - 1\}^{3/2}\eta/kc^2 \cdot 1/2\omega^2 \\
&\quad \cdot \partial^2 a_0/\partial T^2 \cdot (\omega\tau_1)^2, \\
c_2 &= 3\{(cT')^2 - 1\}^{1/2} cT'\eta/kc^2 \cdot 1/\omega \\
&\quad \cdot \partial a_0/\partial T \cdot c\tau_1'\omega\tau_1, \\
c_3 &= 3\{(cT')^2 - 1/2\}\{(cT')^2 - 1\}^{-1/2}\eta a_0/kc^2 \\
&\quad \cdot (c\tau_1')^2, \\
c_4 &= -1/4 \cdot \{(cT')^2 - 1\}^{3/2}\eta/kc^2 \cdot 1/k^2 \\
&\quad \cdot (\partial^2 a_0/\partial z^2 + k^2 a_0)(kr_1)^2, \\
c_5 &= 1/2 \cdot \{(cT')^2 - 1\}^{1/2}\eta/kc^2 \\
&\quad \cdot (1/k \cdot \partial a_0/\partial z + cT' \cdot 1/\omega \cdot \partial a_0/\partial T) kr_1 r_1', \\
c_6 &= -1/2 \cdot \{(cT')^2 - 1\}^{1/2}\eta a_0/kc^2 \cdot r_1'^2, \\
&1/k \cdot r_2'' - \{(cT')^2 - 1\}^{1/2}\eta/kc^2 \cdot \{cT' a_0 r_2' + 1/2 \\
&\quad \cdot (cT'\partial a_0/\partial z + \partial a_0/\partial T \cdot 1/c) r_2\} = \sum_{j=1}^{4} d_j, \qquad (16)
\end{aligned}
$$

where

$$
\begin{aligned}
d_1 &= 1/2 \cdot \{(cT')^2 - 1\}^{1/2}\eta/kc^2 \cdot (1/\omega^2 \cdot \partial^2 a_0/\partial T^2 \\
&\quad + cT' \cdot 1/\omega k \cdot \partial^2 a_0/\partial z \partial T)\omega\tau_1 kr_1, \\
d_2 &= \{(cT')^2 - 1\}^{-1/2}\eta/kc^2 \cdot [1/2 \cdot cT' \cdot 1/\omega \\
&\quad \cdot \partial a_0/\partial T + \{(cT')^2 - 1/2\} \\
&\quad \cdot 1/k \cdot \partial a_0/\partial z] c\tau_1' kr_1, \qquad (17) \\
d_3 &= \{(cT')^2 - 1\}^{1/2} cT'\eta/kc^2 \cdot 1/\omega \\
&\quad \cdot \partial a_0/\partial T \cdot \omega\tau_1 r_1', \\
d_4 &= 2\{(cT')^2 - 1\}^{-1/2}\{(cT')^2 - 1/2\}\eta a_0/kc^2 \\
&\quad \cdot c\tau_1' r_1'.
\end{aligned}
$$

3 REPRESENTATION OF SECOND-ORDER ABERRATION

The left-hand sides of Eqs. (14) and (16) have just the same forms as those of the paraxial trajectory equations (10) and (11) respectively; the right-hand sides of them characterize the second-order equations and are composed of the quadratic terms of the paraxial variables.

The second-order longitudinal aberrations at an arbitrary point z are represented as a function of the paraxial variables at the injection plane by the following expression:

$$
\begin{pmatrix} c\tau_2' \\ \omega\tau_2 \end{pmatrix} = \begin{pmatrix} T'_{0020} & T'_{0011} & T'_{0002} & T'_{2000} & T'_{1100} & T'_{0200} \\ T_{0020} & T_{0011} & T_{0002} & T_{2000} & T_{1100} & T_{0200} \end{pmatrix} \underset{\sim}{g}, \qquad (18)
$$

$$
\underset{\sim}{g} = \{(\omega\tau_{1i})^2, \omega\tau_{1i} c\tau_{1i}', (c\tau_{1i}')^2, (kr_{1i})^2, kr_{1i} r_{1i}', r_{1i}'^2\}^t, \qquad (19)
$$

where $\{\cdots\}^t$ means the transpose matrix of $\{\cdots\}$. T'_{klmn} and T_{klmn} are the second-order longitudinal aberration coefficients. The subscripts k, l, m, n indicate the exponents of the terms

$$
(kr_{1i})^k r_{1i}'^l (\omega\tau_{1i})^m (c\tau_{1i}')^n;
$$

for example $T'_{0011}(\omega\tau_{1i})^1(c\tau_{1i}')^1$.†

We can calculate the values of T_{klmn} and T'_{klmn} in the same way as (L_{jk}) or (M_{jk}). The value of T_{0020}, for instance is equal to the solution $\omega\tau_2$ of Eq. (14) under the injection condition of $kr_{1i} = 0$, $r_{1i}' = 0$, $\omega\tau_{1i} = 1$ and $c\tau_{1i}' = 0$, and the value of T'_{0020} equal to the derivative of $c\tau_2$. Of course, the paraxial solutions substituted into the right-hand side of Eq. (14) must be subjected to the same injection conditions as the above. The remaining coefficients can be obtained likewise.

Substituting Eqs. (12), (13) and (18) into Eqs. (6) and (7), the first- and the second-order kinetic energy at the exit plane for the optimum injection are given by

$$
K_{1e}/K_{0e} = \kappa_e L_{11} c\tau_{1i}', \qquad (20)
$$

$$
\begin{aligned}
K_{2e}/K_{0e} = {} & \kappa_e T'_{0020}(\omega\tau_{1i})^2 + \kappa_e T'_{0011}\omega\tau_{1i} c\tau_{1i}' \\
& + (\lambda_e L_{11}^2 + \kappa_e T'_{0002})(c\tau_{1i}')^2 \\
& + (\mu_e M_{12}^2 + \kappa_e T'_{2000})(kr_{1i})^2 \\
& + (2\mu_e M_{11} M_{12} + \kappa_e T'_{1100}) kr_{1i} r_{1i}' \\
& + (\mu_e M_{11}^2 + \kappa_e T'_{0200}) r_{1i}'^2, \qquad (21)
\end{aligned}
$$

where the subscript e indicates the exit plane. The subscript e to L_{jk}, M_{jk} and T'_{klmn} is omitted for notational simplicity. From Eqs. (20) and (21), we can estimate the energy variation as a function of the variation of the injection energy (in the 1st order), the injection phase width (in the 2nd order) and the transverse properties of injection beams (in the 2nd order).

The second-order transverse aberrations are represented as follows,

$$
\begin{pmatrix} r_2' \\ kr_2 \end{pmatrix} = \begin{pmatrix} S'_{1010} & S'_{1001} & S'_{0110} & S'_{0101} \\ S_{1010} & S_{1001} & S_{0110} & S_{0101} \end{pmatrix} \underset{\sim}{h}, \qquad (22)
$$

$$
\underset{\sim}{h} = \{kr_{1i}\omega\tau_{1i}, kr_{1i} c\tau_{1i}', r_{1i}'\omega\tau_{1i}, r_{1i}' c\tau_{1i}'\}^t. \qquad (23)
$$

S'_{klmn} and S_{klmn} are the second-order transverse aberration coefficients. These values can be calculated in the same way as T'_{klmn}, T_{klmn}.

† Equation (18) is slightly different from the representation of the aberration coefficients of Ref. 6.

4 INVARIANCE OF LONGITUDINAL EMITTANCE ON Z-AXIS

Let us write the normalized longitudinal emittance[4] as follows,

$$\tilde{\varepsilon}_l \triangleq \oint \Delta K/mc^2 \cdot \delta(\omega \Delta t), \tag{24}$$

where ΔK is the deviation of the kinetic energy from K_0, and $\omega\Delta t$ is the deviation of the phase from ωT. If we put $\Delta K = K_1$ and $\omega\Delta t = \omega\tau_1$ in the above equation (24), $\tilde{\varepsilon}_l$ is invariant along the z-axis.[4]

Now, to the second-order approximation, $\tilde{\varepsilon}_l$ is not invariant in general. It can be shown, however, that for the electrons moving along the z-axis, $\tilde{\varepsilon}_l$ is invariant to the second order, if

$$|\Delta K_{1i}/K_{0i}| \ll |\omega\tau_{1i}|. \tag{25}$$

The above inequality (25) means that the variation of the injection energy is sufficiently smaller than the injection phase width, that is, the longitudinal emittance contour is flat. This condition can be also written as $|c\tau'_{1i}| \ll |\omega\tau_{1i}|$.

The proof is as follows. From Eq. (24), $\tilde{\varepsilon}_l$ in the second-order approximation is given by,

$$\tilde{\varepsilon}_{le} = \oint K_{1e}/mc^2 \cdot \delta(\omega\tau_{1e}) + \oint K_{2e}/mc^2 \cdot \delta(\omega\tau_{1e}) + \oint K_{1e}/mc^2 \cdot \delta(\omega\tau_{2e}). \tag{26}$$

The first term of the right-hand side of the above equation (26) has the same value as the one at the injection plane from the paraxial invariance theorem.[4] If the above assumptions are applied to the last two terms of the right-hand side of Eq. (26), then only the term related with the following integral is left:

$$\oint (\omega\tau_{1i})^2 \delta(\omega\tau_{1i}). \tag{27}$$

This integral is equal to the integral of $1/3 \cdot \delta\{(\omega\tau_{1i})^3\}$ which is identically zero for a closed contour. Thus the paraxial invariance of $\tilde{\varepsilon}_l$ is extended to the second-order approximation in this case.

5 NUMERICAL EXAMPLES

We now apply the general treatments to an electron linac with the 5-cell uniform periodic structure in the $\pi/2$-mode standing-wave operation. The operating conditions of the linac are shown in Table I.[7] In this example, the fundamental and first space harmonics are taken into account; the effect of other space harmonics can be easily taken into account as mentioned in Section 2.

TABLE I

Operating conditions of 5-cell uniform periodic electron linac in $\pi/2$-mode standing-wave operation

Frequency	4 GHz
Phase velocity	$0.5284 \cdot c$
Axial electric field	2 MV/m
Space harmonic of -1st order	0.06 × (0-th order)
Injection energy	50 keV
$\omega T_i = \omega T_{opt}$	$0.2875 \cdot \pi$ rad
Output energy	105.641 keV
ωT_e	$3.5477 \cdot \pi$ rad

The injection phase of the reference trajectory is selected to be the optimum injection phase, which means $L_{12} = 0$ in Eq. (12) and can be searched by integrating Eqs. (8) to (10) numerically step by step.

The values of κ, λ and μ of Eqs. (6) and (7) are calculated as follows,

$$\left.\begin{aligned} \kappa_i &= -0.9505,\ \lambda_i = 0.7091,\ \mu_i = 1.1516, \\ \kappa_e &= -1.4905,\ \lambda_e = 1.8222,\ \mu_e = 1.3315. \end{aligned}\right\} \tag{28}$$

Under these conditions, we obtain the values of the paraxial transformation matrices (L_{jk}), (M_{jk}) and the second-order longitudinal aberration coefficients T'_{klmn}, T_{klmn} at the exit plane by numerical integration of Eqs. (8) to (11) and (14). These values are shown in Table II.

In Table II the second-order transverse aberration coefficients are not shown, since as easily seen from Table II the exit plane in this example is neither the image plane ($M_{21} = 0$) nor the cross-over plane ($M_{22} = 0$) for a transverse trajectory.

Now, let us specify the energy resolution as $|\Delta K_e/K_{0e}| \leq 10^{-4}$, which is required for an electron microscope, and discuss the necessary injection conditions. The output energy resolution as a function of the transverse injection conditions is represented by the last three terms of the right-hand side of Eq. (21). With use of Table II and Eq. (28) this is rewritten as

$$K_{2r} = 0.4135(kr_{1i})^2 + 1.6901 \cdot kr_{1i}r'_{1i} + 2.7225 \cdot r'^2_{1i}. \tag{29}$$

The above equation (29) can be transformed into,

$$K_{2r} = 0.1373(k\tilde{r}_{1i})^2 + 2.9987 \cdot \tilde{r}'^2_{1i}, \tag{30}$$

TABLE II

Paraxial transformation matrices (L_{jk}), (M_{jk}), and second-order longitudinal aberration coefficients T'_{klmn}, T_{klmn} in case of Table I

$L_{11} = 0.4323$	$L_{12} = 0.00000$	$M_{11} = 0.6810$	$M_{12} = -0.0009$
$L_{21} = 2.8147$	$L_{22} = 0.6982$	$M_{21} = 3.9735$	$M_{22} = 0.9797$
$T'_{0020} = 0.1398$	$T'_{0011} = 0.5034$	$T'_{0002} = 0.6209$	
$T'_{2000} = -0.2774$	$T'_{1100} = -1.1350$	$T'_{0200} = -1.4123$	
$T_{0020} = 0.5039$	$T_{0011} = 0.9683$	$T_{0002} = 0.6561$	
$T_{2000} = -0.8830$	$T_{1100} = -2.5890$	$T_{0200} = -2.3786$	

where

$$\begin{aligned} kr_{1i} &= k\tilde{r}_{1i}\cos\xi - \tilde{r}'_{1i}\sin\xi, \\ r'_{1i} &= k\tilde{r}_{1i}\sin\xi + \tilde{r}'_{1i}\cos\xi, \\ \xi &= -0.3159 \text{ rad}. \end{aligned} \tag{31}$$

We see from Eq. (30) that K_{2r} is definitely positive; the off-axis electron has always the larger output energy than that of the axial electron. In order to keep K_{2r} less than 10^{-4}, the following condition must be satisfied:

$$(k\tilde{r}_{1i})^2/(2.6988 \times 10^{-2})^2 + \tilde{r}'^2_{1i}/(0.5775 \times 10^{-2})^2 < 1. \tag{32}$$

The region given by Eq. (32) is shown in Figure 1.

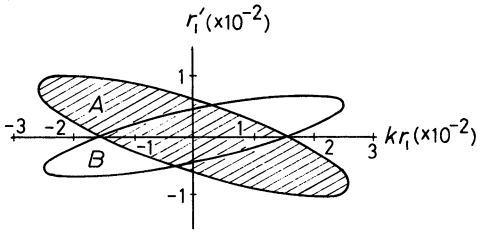

FIGURE 1 Allowed transverse injection conditions to keep energy resolution less than 10^{-4} in case of Table I: *A*. Transformed region at exit plane: *B*.

Furthermore, that at the exit plane is also shown, which is transformed by (M_{jk}).

From Eqs. (20), (21), (25), (28) and Table II, the longitudinal injection conditions which keep the energy resolution less than 10^{-4} are

$$-1.4751 \times 10^{-4} + 0.3074(\omega\tau_{1i})^2 < K_{1i}/K_{0i} < 1.4751 \times 10^{-4} + 0.3074(\omega\tau_{1i})^2. \tag{33}$$

The region given by Eq. (33) is shown in Figure 2. Such a longitudinal property can be realized by chopping the beam into short pulses and/or adjusting the phase of a prebuncher to a decelerating one.

Figure 3 shows the normalized longitudinal emittance contours in case of the reference trajec-

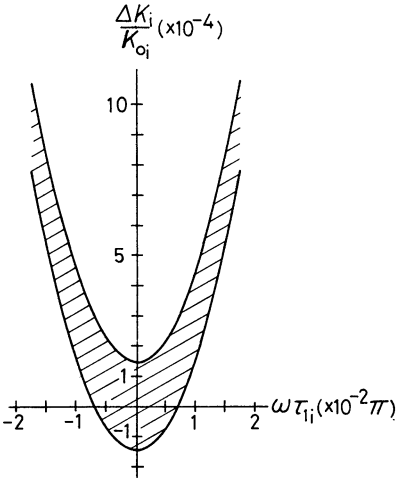

FIGURE 2 Required injection region in longitudinal emittance diagram to keep energy resolution less than 10^{-4} in case of Table I.

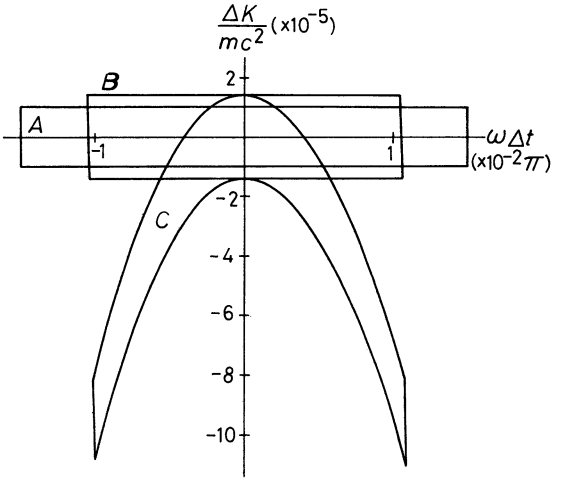

FIGURE 3 Normalized longitudinal emittance contour for axial electrons at optimum injection phase in case of Table I.
A: injection contour,
B: paraxial one at exit plane,
C: *B* corrected by second-order aberration.

tory of Table II. The injection conditions are given by

$$|K_{1i}/mc^2| \leq 10^{-5}, |\omega\tau_{1i}| \leq 1.5\pi \times 10^{-2} \text{ rad}, \quad kr_{1i} = r'_{1i} = 0 \quad (34)$$

and specified by A. The contour B is the paraxial one at the exit plane and the contour C is corrected by the second-order aberration to the contour B.

The area within the contour B is equal to that of the contour A, and the area within the contour C is almost equal to that of the contour A, as mentioned in Section 4.

The emittance diagram for the off-axis electrons can be obtained by shifting Figure 3 upward by $K_{2r}K_{0e}/mc^2$.

6 CONCLUSIONS

We have shown the procedure to estimate the second-order approximation by the aberration coefficients which are calculated from the direct integration of the second-order longitudinal and transverse trajectory equations. The output energy variation is expressed as a function of the injection energy variation (in the 1st order), the injection phase width (in the 2nd order) and the transverse properties of the injection beams (in the 2nd order), when the injection phase is chosen as the optimum value. It is proved that the paraxial invariance of the normalized longitudinal emittance extends to the second-order approximation for the axial electrons if the injection energy variation is sufficiently smaller than the injection phase width. Finally, we have applied this method to a high energy resolution linac, calculated numerically the paraxial transformation matrices and the second-order aberration coefficients at the optimum injection phase, and discussed the second order aberration and the longitudinal emittance.

ACKNOWLEDGEMENT

We are indebted to Dr. J. Matsuda for his useful discussion about the aberration theory of the electron trajectory in rf-fields, and to Mr. S. Kakuno for his help in the computation.

REFERENCES

1. A. Septier and M. Boussoukaya, *Nucl. Inst. Meth.*, **80**, 273 (1970).
2. M. Boussoukaya and A. Septier, *Nucl. Inst. Meth.*, **80**, 109 (1970).
3. M. Boussoukaya and A. Septier, *Particle Accelerators*, **2**, 305 (1971).
4. Y. Takeuchi, H. Fujioka and K. Ura, *Trans., IECE, Japan*, **56-B**, 551 (1973).
5. P. A. Sturrock, *Static and Dynamic Electron Optics* (Cambridge Univ. Press, London, 1955), Chap. 6.
6. J. Katsuda and K. Ura, Optik, **40**, 179, 284 (1974).
7. Y. Takeuchi, H. Fujioka, and K. Ura, Technol. Rep., Osaka Univ., **24**, No. 1168 (1974).

Appendix

The field components E_z, E_r and B_ϕ are expanded from Eq. (3) and Maxwell's equations as follows,

$$E_z(t, r, z) = E_z(T, 0, z) + \tilde{\omega}\partial a_0/\partial T \cdot \tau_1 + \tilde{\omega}^2\{-1/4 \cdot (\partial^2 a_0/\partial z^2 - \varepsilon\mu\partial^2 a_0/\partial T^2)r_1^2 + 1/2 \cdot \partial^2 a_0/\partial T^2 \cdot \tau_1^2 + \partial a_0/\partial T \cdot \tau_2\} + \cdots, \quad (A.1)$$

$$E_r(t, r, z) = \tilde{\omega}(-1/2 \cdot \partial a_0/\partial z \cdot r_1) + \tilde{\omega}^2\{-1/2 \cdot \partial^2 a_0/\partial T\partial z \cdot r_1\tau_1 - 1/2 \cdot \partial a_0/\partial z \cdot r_2\} + \cdots, \quad (A.2)$$

$$B_\phi(t, r, z) = \tilde{\omega}\varepsilon\mu 1/2 \cdot \partial a_0/\partial T \cdot r_1 + \tilde{\omega}^2\varepsilon\mu(1/2 \cdot \partial^2 a_0/\partial T^2 \cdot r_1\tau_1 + 1/2 \cdot \partial a_0/\partial T \cdot r_2) + \cdots, \quad (A.3)$$

where

$$a_0 = E_z(t = T, r = 0, z).$$